



INSTITUTE FOR DEFENSE ANALYSES

Skin Penetration Modeling Limitations and Opportunities

Sujeeta B. Bhatt
Yevgeny Macheret
Jeremy A. Teichman
Jessica G. Swallow

March 2022

Approved for public release;
distribution is unlimited.

IDA Document NS D-33040

Log: H 22-000133

INSTITUTE FOR DEFENSE ANALYSES
730 East Glebe Road
Alexandria, Virginia 22305-3086



The Institute for Defense Analyses is a nonprofit corporation that operates three Federally Funded Research and Development Centers. Its mission is to answer the most challenging U.S. security and science policy questions with objective analysis, leveraging extraordinary scientific, technical, and analytic expertise.

About This Publication

This work was conducted by the IDA Systems and Analyses Center under contract HQ0034-19-D-0001, project DU-2-4273, “IFC Modeling Uncertainty Analysis,” for the Joint Intermediate Force Capabilities Office (JIFCO). The views, opinions, and findings should not be construed as representing the official position of either the Department of Defense or the sponsoring organization.

For More Information

Sujeeta B. Bhatt, Project Leader
sbhatt@ida.org, 703-578-2719

Leonard J. Buckley, Director, Science and Technology Division
lbuckley@ida.org, 703-578-2800

Copyright Notice

© 2022 Institute for Defense Analyses
730 East Glebe Road, Alexandria, Virginia 22305-3086 • (703) 845-2000.

This material may be reproduced by or for the U.S. Government pursuant to the copyright license under the clause at DFARS 252.227-7013 (Feb. 2014).

INSTITUTE FOR DEFENSE ANALYSES

IDA Document NS D-33040

**Skin Penetration Modeling Limitations
and Opportunities**

Sujeeta B. Bhatt
Yevgeny Macheret
Jeremy A. Teichman
Jessica G. Swallow

Introduction

The University of Virginia (UVA) built a model for estimating the risk of significant injury due to skin penetration.¹ They undertook a number of steps in order to build this model. Specifically, UVA:

1. Built a finite-element model (FEM) to simulate the dynamic effects of blunt impact projectiles on the skin.
2. Conducted post-mortem human-subject (PMHS) experiments to measure injury occurrence under different velocity impacts from a set of rigid projectiles.
3. Created a response-surface model (“injury risk function” (IRF)), a linear best-fit surface, to estimate risk of injury based on the PMHS experiments to account for the various independent variables.
4. Developed a correlation between FEM results (in this case, the 95th percentile maximum principal strain (MPS-95) is the selected value extracted from the FEM simulation) and the IRF to produce a curve of MPS-95 vs. injury risk. In doing so, they unified all of the input parameters of the IRF into a single parameter determining the risk of injury, a sole value upon which the probability of injury depends, the MPS-95.
5. Conducted experiments to investigate whether future projectiles can be characterized with respect to injury probability using ovine specimens as a surrogate for human (PMHS) testing. Note, we do not analyze the ovine portion of the UVA research in this document.

In this document, we characterize some shortcomings and limitations of the UVA model as it is expected to be implemented by the Johns Hopkins University Applied Physics Laboratory (JHU/APL) based both on theoretical considerations of their model construct and on their own experimental results. We also suggest a number of potential future enhancements to improve the accuracy of the model predictions.

Injury Correlation Derivation/Employment Mismatch

An *injury correlation* is a functional relationship between a biophysical response variable (the *injury correlate*) and the probability of injury. For each value of the injury correlate there is a one-to-one relationship (the correlation) providing the probability of injury. In this case, UVA developed an injury correlation using MPS-95 (computed by the FEM) as the correlate, leading to the following injury correlation:

¹ D. Shedd et al., “Skin Penetration from Non-Lethal Munitions,” Final Technical Report, UVA Center for Applied Biomechanics, September 2021

$$\text{Probability of injury} = f(\text{MPS-95})$$

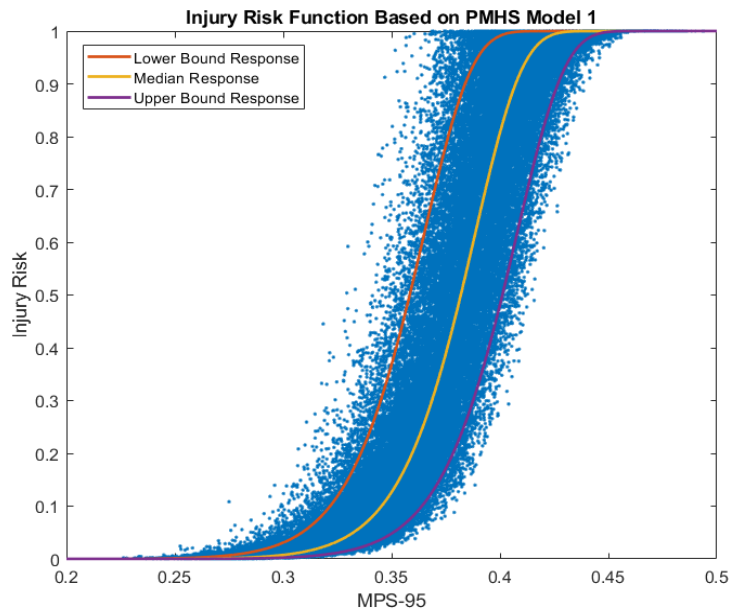


Figure 1. UVA Final Report Figure 63: Lower bound, median, and upper bound injury risk functions (IRFs) relating MPS-95 to injury risk.

Determining Injury Response Function (IRF)

UVA generated the injury correlation (the yellow curve in Figure 1) by conducting PMHS experiments to measure injury occurrence under different velocity impacts from a set of rigid projectiles. They built a response surface model (IRF) to estimate risk of injury based on those experiments accounting for various independent variables (velocity, diameter, shape, and skin thickness) as shown in Figure 2. UVA generated a correlation between the FEM results (MPS-95) and the IRF to produce a curve of MPS-95 vs. injury risk.

Determining Skin Deformation (MPS-95) via “Metamodel”

Rather than evaluating the FEM at all relevant impact conditions, UVA built a metamodel (a quadratic-fit response surface), as shown in Figure 3, to predict the FEM-computed MPS-95 as a function of impactor velocity and diameter, and shape and skin and adipose tissue stiffness, holding skin thickness constant at 2 mm.

Correlating IRF and MPS-95

UVA then used the metamodel to predict MPS-95 for a variety of impactors, impact velocities, and statistically varying skin and adipose tissue stiffnesses, as shown on the left-hand side of Figure 4. The IRF was evaluated for the same conditions as shown on the right-hand side of Figure 4 giving a probability of injury corresponding to each computed

MPS-95. The IRF/MPS-95 pairs are shown as blue dots in Figure 1. The injury correlation at the bottom of Figure 4 is the best-fit Weibull survival curve to these MPS-95/probability-of-injury pairs; it is shown as a yellow curve in Figure 1. The IRF/MPS-95 pairs do not all fall nicely onto the yellow curve for a number of reasons, as discussed below.

Model Employment vs. Model Development

In order to employ this construct consistently, the injury curve has to be applied in the same fashion in which it was derived. In other words, for a given impactor and impact velocity, a series of MPS-95s based on statistically varying skin and adipose tissue stiffness have to be computed, as was done to compute the blue points in Figure 1. For each of those MPS-95 values, one would want to evaluate the injury correlation to come up with a tissue-property-specific probability of injury. These probabilities of injury would then be averaged to find the overall probability of injury over the population of tissue properties in much the same fashion that the yellow curve was derived as a best fit over the blue dots. UVA originally envisioned doing so—consistently using the correlation by running multiple FEM simulations with varying tissue stiffnesses. JHU/APL, for computational efficiency, intends to run only a single FEM simulation for each impact with fixed tissue properties.

Thus, there appears to be an inconsistency between JHU/APL’s planned use of UVA’s proposed injury correlation and the method UVA used to construct that correlation. Due to the computational burden, JHU/APL intends to use their risk of significant injury (RSI) prediction tool and run the FEM simulation once for each impact condition and location using a fixed stiffness for the skin and adipose tissue. The tool will compute a single MPS-95 for each impact based on the FEM output and evaluate the injury correlation (probability of injury vs. MPS-95 represented by the yellow curve in Figure 1) from UVA, which is based on varying tissue stiffness, to come up with the probability of injury. As it stands, the JHU/APL plan, as shown in Figure 5, assumes that evaluating the injury correlation once based on an average set of properties is equivalent to averaging the probabilities of injury for a distribution of properties. In general, this is not true and could introduce errors.

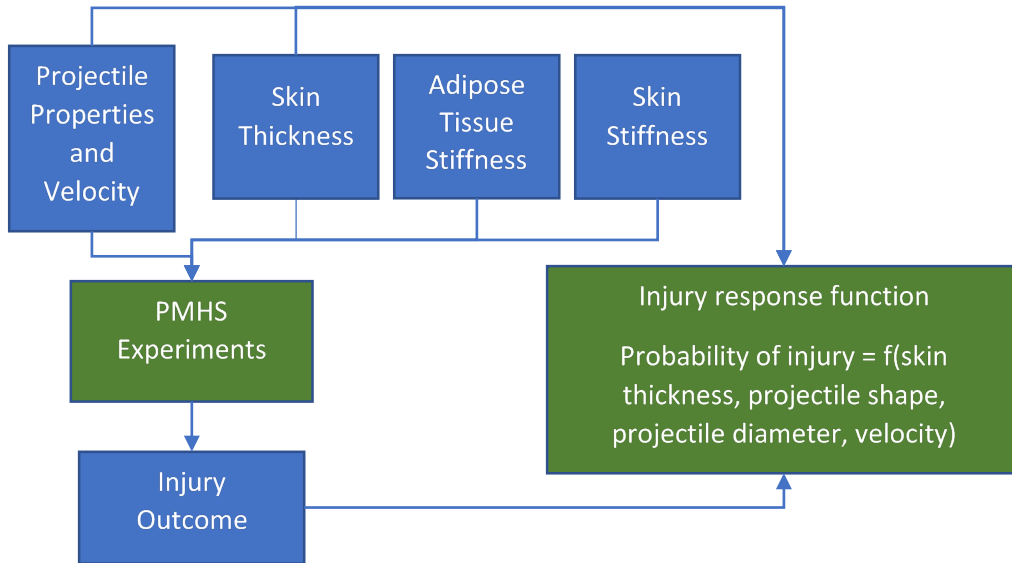


Figure 2. Injury response function derivation. Variable inputs and outputs are shown in blue and functional blocks in green.

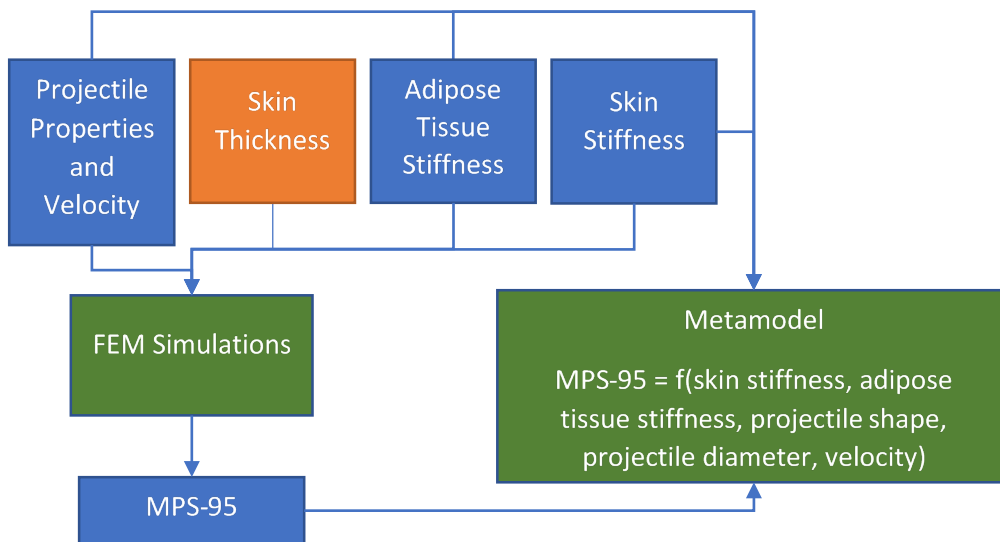


Figure 3. Metamodel derivation. Variable inputs and outputs are shown in blue, fixed inputs in orange, and functional blocks in green.

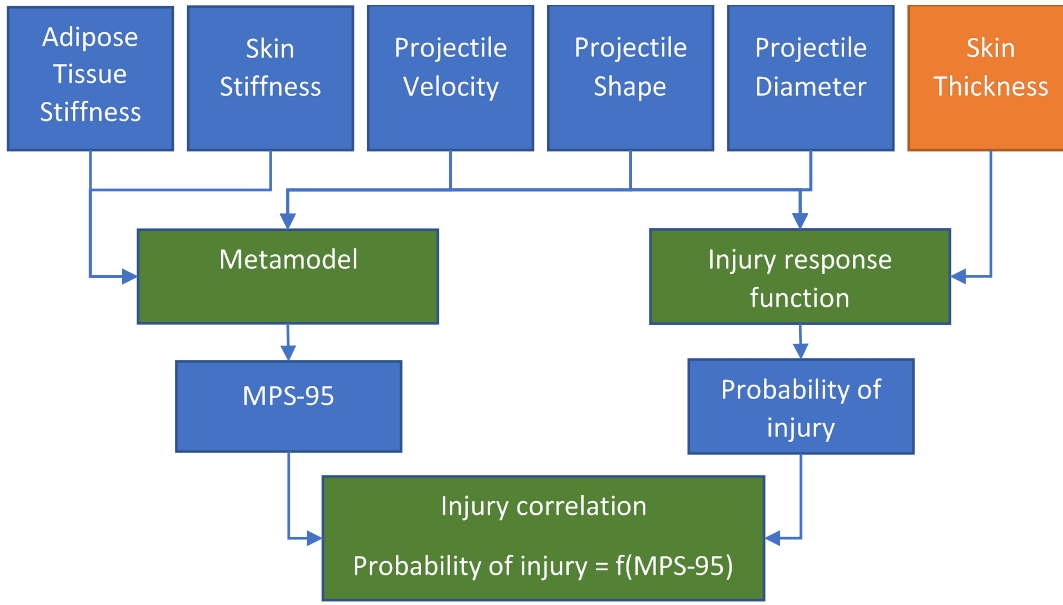


Figure 4. Injury correlation derivation. In UVA’s derivation of the injury correlation, the two tissue stiffnesses (top left) are randomly drawn from a statistical distribution, and the skin thickness (top right) is fixed at 2 mm. Variable inputs and outputs are shown in blue, fixed inputs in orange, and functional blocks in green.

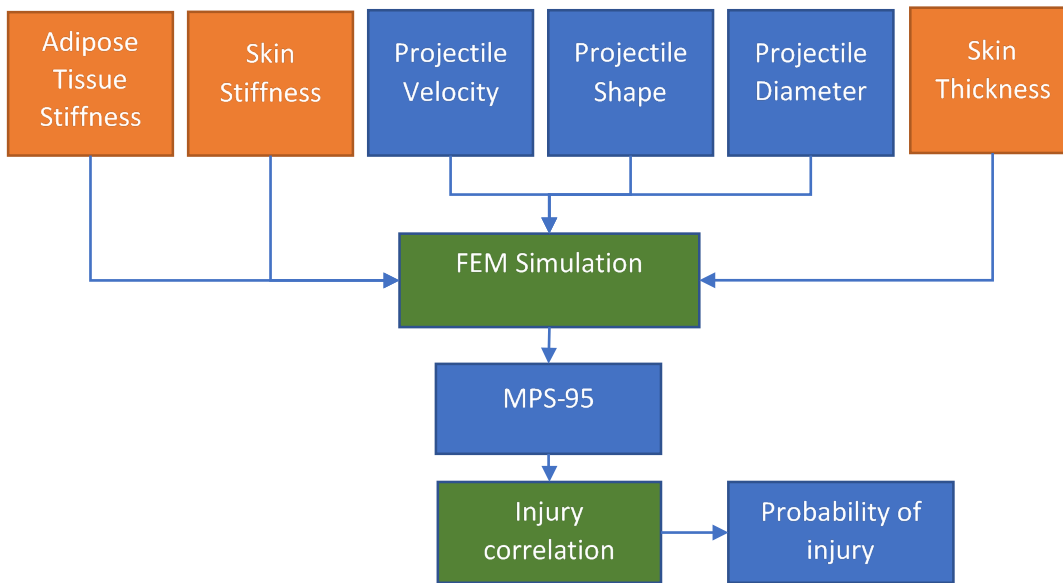


Figure 5. Injury correlation use. In JHU/APL’s intended use, the two tissue stiffnesses (top left) are fixed at their mean values. Variable inputs and outputs are shown in blue, fixed inputs in orange, and functional blocks in green.

When employing JHU/APL’s RSI evaluation methodology, it would be more appropriate to use an injury correlation derived using fixed tissue stiffnesses rather than statistically varying tissue stiffnesses as in the yellow curve in Figure 1. This would be

equivalent to recoloring the two top left boxes in Figure 4 orange indicating that the injury correlation would be derived based on fixed values (mean) of skin and adipose tissue stiffness. The quick-running metamodel could readily be run with fixed rather than statistically varying properties to generate a new scatter-plot analogous to Figure 1 with an associated new best-fit injury correlation. UVA did this and the results are shown in Figure 6 as orange dots overlaid on the blue dots of Figure 1. The replacement injury correlation would be the best fit to the orange dots in Figure 6.

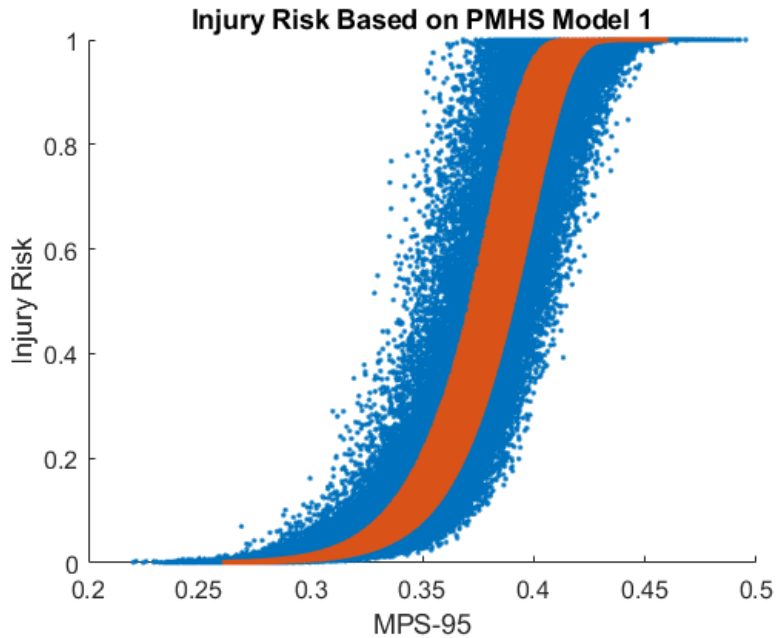


Figure 6. UVA final report Figure 64: Injury risk variation when considering variation in both tissue mechanical properties and impactor design (blue) and considering variation in only impactor design (orange).

As can be observed in Figure 7, the best-fit curve may not change much, but the scatter is considerably reduced. It turns out this inconsistency in the best fit curve may be small compared to other sources of error in the probability of injury, as will become clear in the detailed discussion of sources of uncertainty. Nevertheless, this inconsistency is easily avoided. Note that because the IRF does not have tissue stiffness as an input variable, evaluating the metamodel using fixed tissue properties exclusively reduces horizontal scatter of the points while retaining their vertical positions. In other words, one impact condition would lead to many different MPS-95 values due to differences in tissue properties. Vertical spread is due to the fact that different projectile/velocity combinations could lead to the same MPS-95. Although the larger scatter of the blue points may represent true variation of the human experience of MPS-95, the goal of the prediction tool is to estimate the population-wide risk of injury, not the variation in injury risk from individual to individual.

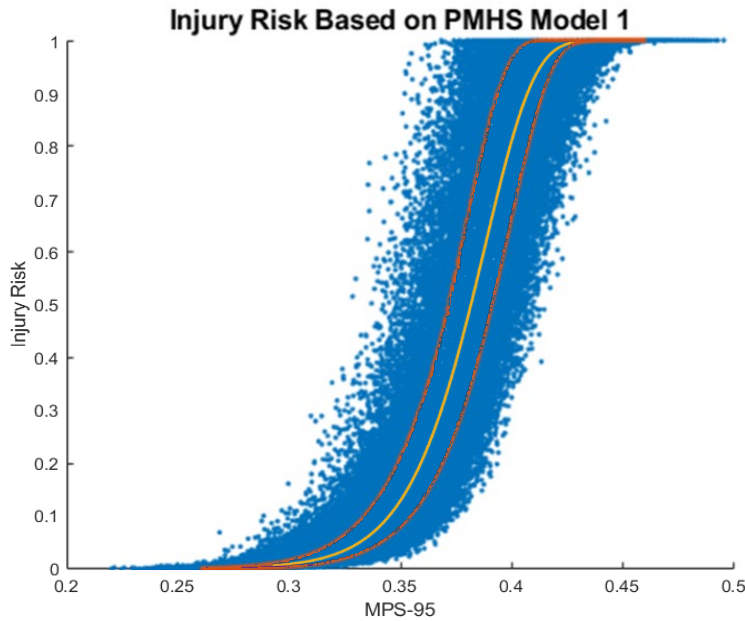


Figure 7. Superposition of Figure 1 and Figure 6 showing the best fit injury correlation for the blue points juxtaposed with the outline of the region of orange points from Figure 6.

Other Uncertainty Factors

Data in Figure 1 and Figure 6 indicate that MPS-95 correlates well with injury risk. However, the data show considerable scatter about the mean trend. For instance, even if one computed the MPS-95 with great accuracy, the scatter suggests that the level of uncertainty in injury risk could vary over a nearly 30% span in some regions even if the orange points in Figure 6 are used. Is this irreducible and does it represent the true uncertainty?

Other potential sources of uncertainty include modeling error (i.e., does the MPS-95 computed in the FEM simulation accurately represent the maximum principal strain experience by a live human target), and correlation error (e.g., MPS-95 not being the correct or sole correlate of skin penetration injury).

Modeling Error

The FEM simulation calculates MPS-95 as follows. UVA's computation first takes the maximum over time of the principle strain in each element in a defined region around the impact point. Then it calculates the 95th percentile of those values across the elements in the defined impact region. The UVA FEM models the outer layers of soft tissue of the body in three layers, each with its own set of properties. The adipose tissue and muscle are each modeled as volume elements. The skin is modeled as a two-dimensional (2-D) shell element. Each layer has uniform properties across the entire body. In particular, the modeled skin has uniform thickness throughout the body.

If MPS-95 is indeed the single or principal correlate of skin penetration injury, then factors influencing injury risk should also influence MPS-95. Skin thickness variation across the body, which UVA found in its PMHS experiments to be a sensitive determinant of injury, see [9], would be expected to give rise to significantly different values of MPS-95. As shown in Figure 9, the injury risk for a fixed projectile and impact velocity systematically varies with regional skin thickness around the body to a degree far larger than the scatter in the orange dots in Figure 6. This directly suggests that the apparent uncertainty in the single injury correlation curve is small compared to actual systematic body region variation. A location along the x-axis in Figure 8 and Figure 9 dictates a single impact condition, which would lead to a single MPS-95 value. Figure 9 indicates that there may be as much as 60% systematic variation in probability of injury from body region to body region for a single impact condition.

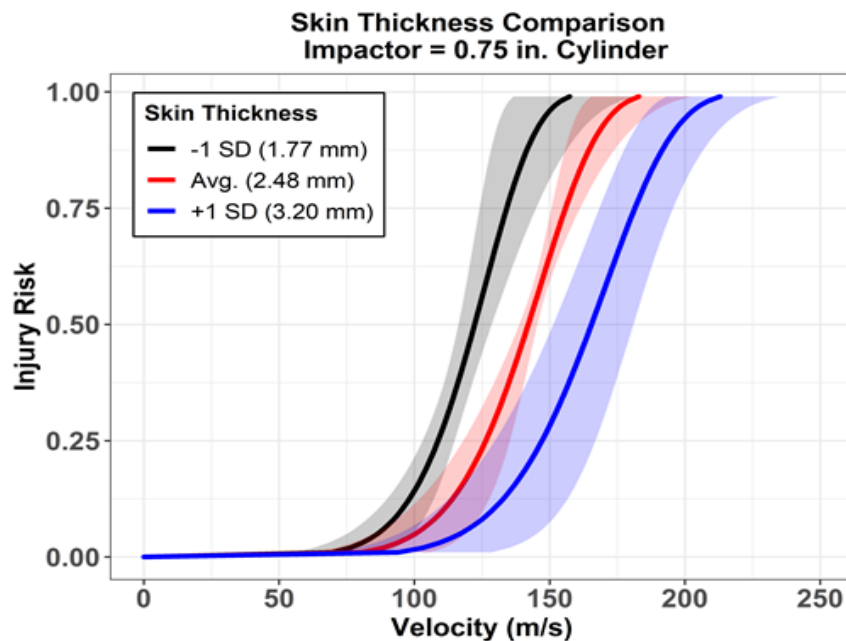


Figure 8. UVA final report Figure 13: The effects of overall skin thickness variations on the PMHS IRF response. The IRF response was predicted for the 0.75 in. cylinder impactor at three skin thickness levels (1.77 mm, 2.48 mm, and 3.20 mm) representing the mean thickness (± 1 SD) for the six PMHS. The corridors represent the 95% confidence intervals for each predicted response.

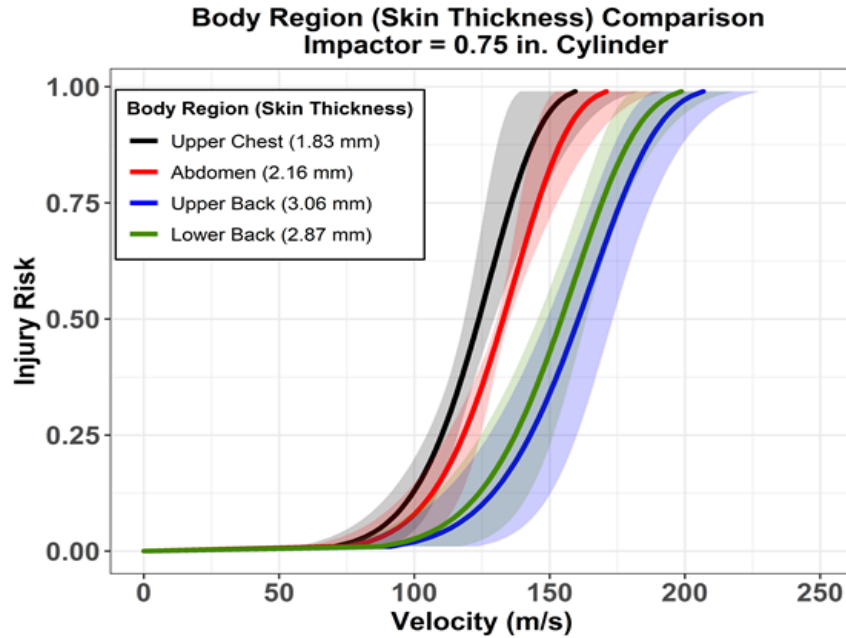


Figure 9. UVA final report Figure 14: The effects of regional skin thickness variations on the PMHS IRF response. The IRF response was predicted for the 0.75 in. cylinder impactor at four skin thickness levels (1.83 mm, 2.16 mm, 3.06 mm, and 2.87 mm) representing the mean thickness for the Upper Chest, Abdomen, Upper Back, and Lower Back, respectively. The corridors represent the 95% confidence intervals for each predicted response.

The probability of injury predicted by one skin thickness curve may have very different operational implications than another. One could think of the skin thickness variation in the context of Figure 6. Consideration of population skin thickness variation in the IRF, as much as UVA had considered skin and adipose tissue stiffness in the metamodel, would contribute to significantly larger vertical scatter in the blue points. If, in the future, JIFCO utilizes an employment model more along the lines originally envisioned by UVA, statistically varying skin thickness over the population might be at least as important as varying tissue stiffness. For fixed tissue properties (at the population mean), varying the skin thickness by region in the IRF might produce four distinct orange bands in Figure 6 corresponding to regionally distinct injury correlations for a fixed skin thickness FEM. Ideally, considering regional variation in skin thickness in the FEM would reunite these regional correlations to produce a single universal MPS-95 vs. probability of injury curve.

Figure 10 illustrates inconsistencies between experimental data and FEA predictions associated with skin thickness. It shows the MPS-95 for given impactor and impact conditions for four distinct impact locations. Each impact location has a mean anatomical skin thickness shown in the legend and caption of Figure 9. As shown in Figure 9, the injury risk is a decreasing function of skin thickness over the four body regions. Thus, we would expect that MPS-95 in Figure 10 would also be a decreasing function of skin

thickness for each set of conditions. Inspection of Figure 10 shows otherwise. Sometimes, as in the upper-right-hand panel, the thinnest skin (upper chest) corresponds to the highest MPS-95. Other times, as in the upper-left-hand panel, the thinnest skin corresponds to the lowest MPS-95. Other factors influencing MPS-95 differences between the body regions could include local body geometry and anatomy. However, due to the strong sensitivity to skin thickness, we hypothesize that recalculation of Figure 10 with correct anatomical skin thickness in the FEM calculation could re-sort the points into an MPS-95 order more consistently opposite the corresponding skin thickness order.

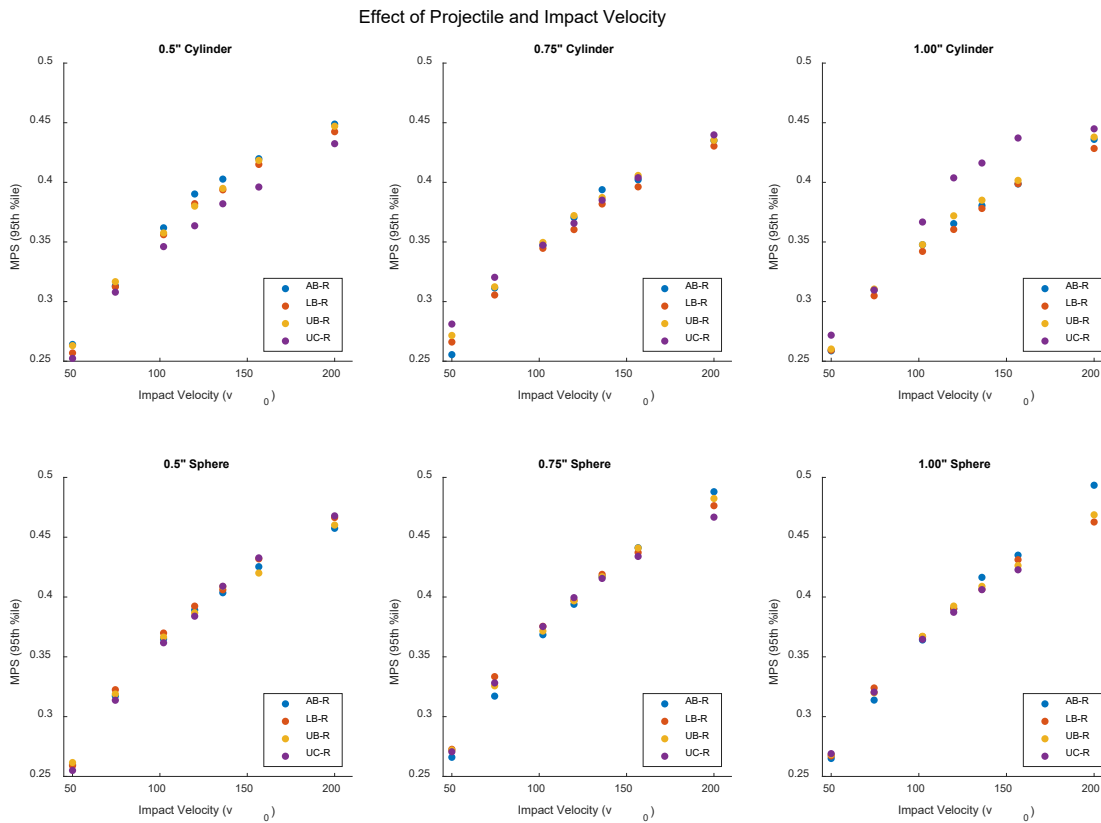


Figure 10. UVA Final Report Figure 51: Effect of impact velocity and impactor geometry. Impacts were conducted at the AB-R [Abdomen], UC-R [Upper chest], UB-R [Upper back], and LB-R [Lower back] impact locations.

RSI Model Accuracy for Different Skin Thickness

Another way to visualize the consistency of the model is shown in Figure 11. It shows the experimental predictions vs. the model predictions for probability of injury. In a perfect world, the points would fall on the diagonal line indicating complete agreement of the model and experiments. Experiments are expected to exhibit scatter but ideally exhibit little bias, particularly since they are the same experiments upon which the model is built. The points in Figure 11 are pretty far off the line. The direction from the points to the line

points in Figure 11 are pretty far off the line. The direction from the points to the line representing perfect agreement between the model and experiments is consistent with correcting skin thickness effects in the FEM. The injury correlation is built from FEM simulations with a single skin thickness (2 mm), meaning the MPS-95 being computed is likely to be biased based on the offset between the true skin thickness and that in the FEM. In regions with anatomical skin thickness larger than that (2 mm) in the FEM, the FEM will likely over-estimate MPS-95 and thence probability of injury and vice versa. Figure 11 demonstrates this effect. The largest over-estimation of injury by the model occurs in the upper back where the anatomical skin thickness furthest exceeds the FEM skin thickness. The biases for the other body regions are also consistent. The second and third largest positive biases occur for the second and third largest positive discrepancies of anatomical vs. model skin thickness (lower back and abdomen); the under-prediction of risk occurs in the upper chest where the model skin thickness exceeds the anatomical skin thickness. Presumably, adjusting the FEM skin thicknesses from their nominal value of 2 mm to anatomical mean values would reduce the observed bias bringing all the points closer to the dashed line. Additionally, bringing the FEM-calculated MPS-95 closer to true MPS-95 would lead to skin penetration injury being more extensible to other body regions beyond those considered here, such as the extremities or head. In other body regions, continuing to utilize only the fixed nominal skin thickness would lead to uncontrolled region-specific biases making extension of the current prediction method to those regions error-prone.

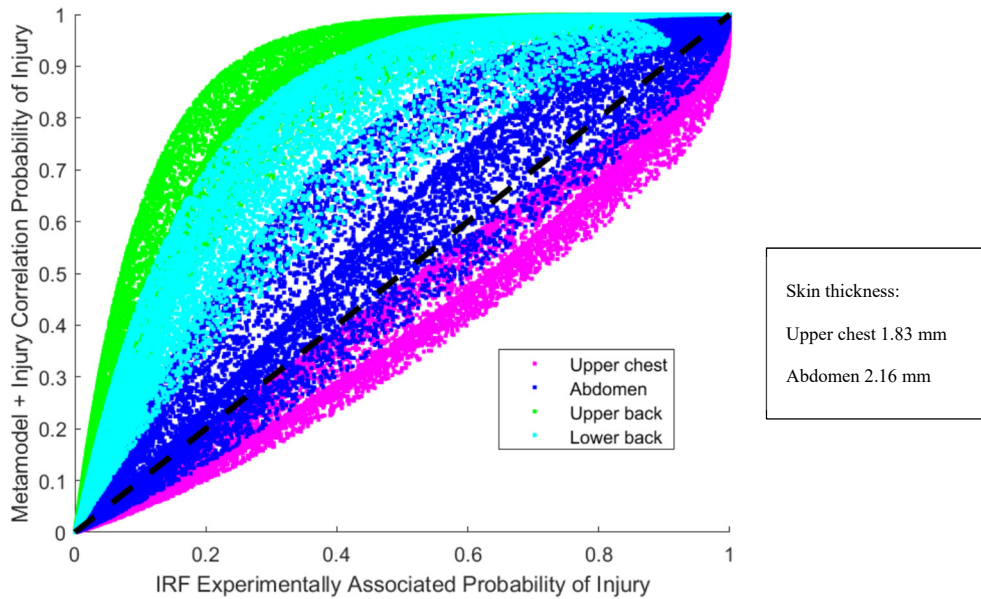


Figure 11. Experiment vs. model. The dashed line shows perfect correlation of experimental injury predictions from the injury response function (IRF) and FEM-derived injury predictions from the metamodel and injury correlation. The points represent 100,000 Monte Carlo runs

varying the projectile shape (sphere or cylinder), diameter (0.5"-1"), velocity (25-175 m/s), and body impact region (upper chest, abdomen, upper back, lower back). For each point, the x-value is computed using the body-region-specific mean skin thickness in the IRF, and the y-value is computed using MPS-95 computed from body-region-specific metamodel from UVA and the generic injury correlation between MPS-95 and probability of injury.

Skin thickness variation is not the only source of potential error in calculation of injury risk or MPS-95. The computational procedure used to calculate MPS-95 creates spatial smoothing effects. To some degree, this is a deliberate outcome to avoid spurious local spikes in computed strains due to discretization and numerical effects. There are also discrepancies between the physical world and the FEM geometry, properties, and computation, which may lead to errors in MPS-95 calculation. UVA conducted grid convergence studies to minimize some of the discretization errors. However, differences between utilized tissue properties and in-vivo tissue properties could lead to MPS-95 computation errors. Skin is currently modeled with behavior derived principally from tensile testing with laboratory tissue coupons. Based on its microstructure, skin would be expected to behave considerably differently in tension and compression. If compressive and shear responses contribute significantly to MPS-95 or to alternate failure mechanisms (and their associated correlates), this could introduce modeling errors in simulated skin behavior. Appendix A addresses potential tissue property and property testing issues as well as skin mechanics in greater detail. Anatomical skin is a 3-D structure, but the FEM treats it as a shell element. Shell elements do not allow arbitrary 3-D states of stress. If realistic stress states differ considerably from what is allowed by the shell model, the stress and strain may not be calculated accurately, directly leading to errors in the computed MPS-95. Note that systematic under or overestimation of MPS-95 would, if consistent, be at least partially compensated for in the injury correlation—any surrogate variable with a one-to-one relationship with MPS-95 could serve equally well as an injury correlate.

Another possible source of modeling error is that in the IRF. Injury risk may not be calculated accurately due to the following:

1. Experimental error in the PMHS studies (e.g., incorrect determination of injury)
2. Systematic discrepancy between PMHS and live targets in tissue properties
3. Effects of clothing (PMHS study did not account for clothing)
4. Inadequate sampling (PMHS subjects systematically differ from target population or fail to adequately capture variation in the target population)

Model results could also be imprecise outside the validation region of the experiments. For instance, the experiments were all done with a limited set of rigid projectiles. Extrapolating to soft projectiles could introduce errors. It has not been experimentally confirmed that MPS-95 is a good injury correlate for soft projectile impact. Nor is it obvious that the same simplifications made in the FEM for rigid impactors will be equally applicable to soft ones. Validation tests with soft projectiles would be important

before relying on the existing model for compliant projectiles. UVA reported work on ovine subjects as human surrogates for penetrating injuries. Perhaps a set of ovine experiments with compliant projectiles could play a part in supporting extension of the model beyond rigid impactors.

Correlation Error

There is a second source of scatter in Figure 6. Different impact conditions can lead to the same MPS-95, and different impact conditions can lead to the same injury risk (e.g., higher velocity but smaller impactor). However, the set of impact conditions leading to identical MPS-95 may not be the same as the set of impact conditions leading to identical injury risk. If MPS-95 were a perfect surrogate for injury risk, the two sets would be expected to be identical because each MPS-95 would lead to only one risk of injury. But if the computed MPS-95 is not a perfect surrogate for injury risk then a single MPS-95 could correspond to multiple possible injury risks. There are a number of reasons why the one-to-one relationship of MPS-95 to injury risk could break down. The previous section covered the possibility that the MPS-95 is not calculated accurately (either in the FEM or the metamodel) or that injury risk is not calculated accurately. It is also possible that either MPS-95 is not the sole correlate of injury risk (other factors independently contribute) or that MPS-95 is not the correct correlate (it is associated but not causative).

Some of the scientific literature suggest that strain energy may be the correct causative predictor of skin rupture. More detail on the mechanics of skin failure and appropriate correlates can be found in Appendix A.

Review and Summary of Current Limitations and Remedies

1. The UVA model uses MPS-95 as a skin injury correlate, while open literature publications report that a maximum strain energy criterion is the most likely skin injury correlate. These two are not always strictly correlated. For example, holding strain constant along one axis and increasing it along another will increase strain energy without changing MPS-95. There may be computational advantages to MPS-95, but it would be worthwhile to evaluate strain energy as a candidate. Strain energy could be computed under similar conditions to MPS-95 employing spatial smoothing and temporal maxima.
2. Extrapolating model results from rigid to soft projectiles may be error-prone. Experiments have not confirmed that MPS-95 is a good injury correlate for soft projectile impact. Nor is it clear that the same simplifications made in the FEM for rigid impactors are valid for soft ones. Validation tests with soft projectiles would be important before extrapolating the existing model. Perhaps this would be useful exploitation of UVA's work establishing ovine surrogates.

3. Open literature publications report skin injury data obtained under tensile loading conditions. Given the complex skin structure and possible tear mechanics (see Appendix A), these may not be applicable for situations where compressive and shear stresses are present as in the blunt impact scenario. Additional experiments could be warranted to improve knowledge of skin behavior and failure under compressive and shear loading. UVA's final report references unpublished results associated with initial exploration of these effects.
4. The FEM uses shell elements for skin, a simplification that does not adequately account for the skin thickness. Regional skin thickness variation was not incorporated into the FEM. Yet, test data show that skin thickness is the strongest skin failure correlate. We recommend regional skin thickness variation (if not full anatomical variation) and its effects be incorporated into the FEM. One way to account for the effect of skin thickness with shell elements is to treat thicker skin as having a higher stiffness. However, our understanding suggests that skin thickness is at least partially incorporated into shell elements. Although the elements may possess no geometrical thickness, the bending and stretching stiffnesses of the elements must incorporate a thickness to translate material properties into element responses. The nominal thickness could thus be used to implement the mechanical effects of variations of skin thickness between different body regions and the effect on deformation and failure. Because the nominal thickness of shell elements is not accompanied by a geometrical thickness, the usual challenges of remeshing due to geometry variation is absent. Thus, it should be comparatively easy to incorporate regional skin thickness variation.
5. Shell elements also do not account for all relevant stress and strain conditions. Test data indicate that rigid projectiles lead to failures at the projectile edges, where through-thickness compressive and shear stresses and strains exist, making it likely that different failure modes are likely as compared to those under pure tensile loading. Shell elements do not allow for lateral strain due to through-thickness compression. Maximum strain energy would be expected to increase under the compression of a projectile leading to earlier failure for higher compressive force. MPS would also be expected to change under the influence of through-thickness compression. Changing to solid elements for the skin would address some of these issues, but would add to computational complexity, potentially detract from stability, and add concerns about meshing and anatomical fidelity.

Here, in order of increasing complexity and increasing fidelity, are ways in which the current construct could be improved with respect to incorporating the effect of skin

thickness. Approaches 1–3 can be incorporated rapidly using the existing metamodel and IRF. Approach 4 requires new simulations using a modified FEM to generate a new metamodel.

1. A future study could statistically vary the skin thickness in the IRF. The study would use fixed mean values for skin and adipose tissue stiffness, in keeping with the current plan for calculating RSI. The skin thickness would be varied statistically representing experiments across a population and generating a larger vertical scatter in the equivalent plot of Figure 6. A new best-fit injury correlation would be generated. This would account for population variation in skin thickness without changing the proposed correlate or requiring extra FEM simulations to employ it. The rerun models using the UVA-reported skin thickness variations in their PMHS of 2.48 ± 0.71 mm are shown in Figure 12.

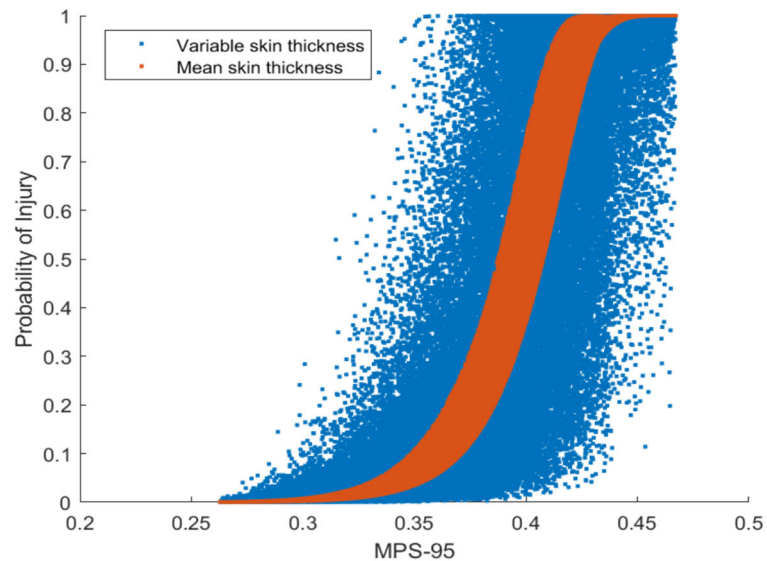


Figure 12. Injury risk vs. MPS-95. IRF based on stochastic skin thickness. The orange points are calculated just as done by UVA in Figure 6, but the vertical position of each dot is computed using the IRF with a fixed skin thickness equal to the mean PMHS anatomical value of 2.48 mm rather than the FEM skin thickness of 2 mm. The blue points are the same except with the skin thickness for each of the 100,000 Monte Carlo runs randomly selected from a normal distribution with a mean of 2.48 mm and a standard deviation of 0.71 mm.

2. Generate region-specific injury correlations based on the mean skin thickness in each of the four considered torso regions. To do so, the IRF would be evaluated deterministically based on the mean skin thickness in the relevant body region, and the metamodel would be evaluated based on deterministic mean values for skin and adipose tissue stiffness resulting in a scatterplot like Figure 6 for each body region. A separate injury correlation for each body region would be fit

based on the associated scatterplot. This would account for body region skin thickness variation in experiments and avoid the error of assuming consistent MPS-95 calculation across body regions inherent in using a FEM with uniform skin thickness. UVA has done this. The rerun models are shown in Figure 13 along with UVA's generic and region-specific injury correlations, and the improved prediction is shown in Figure 14.

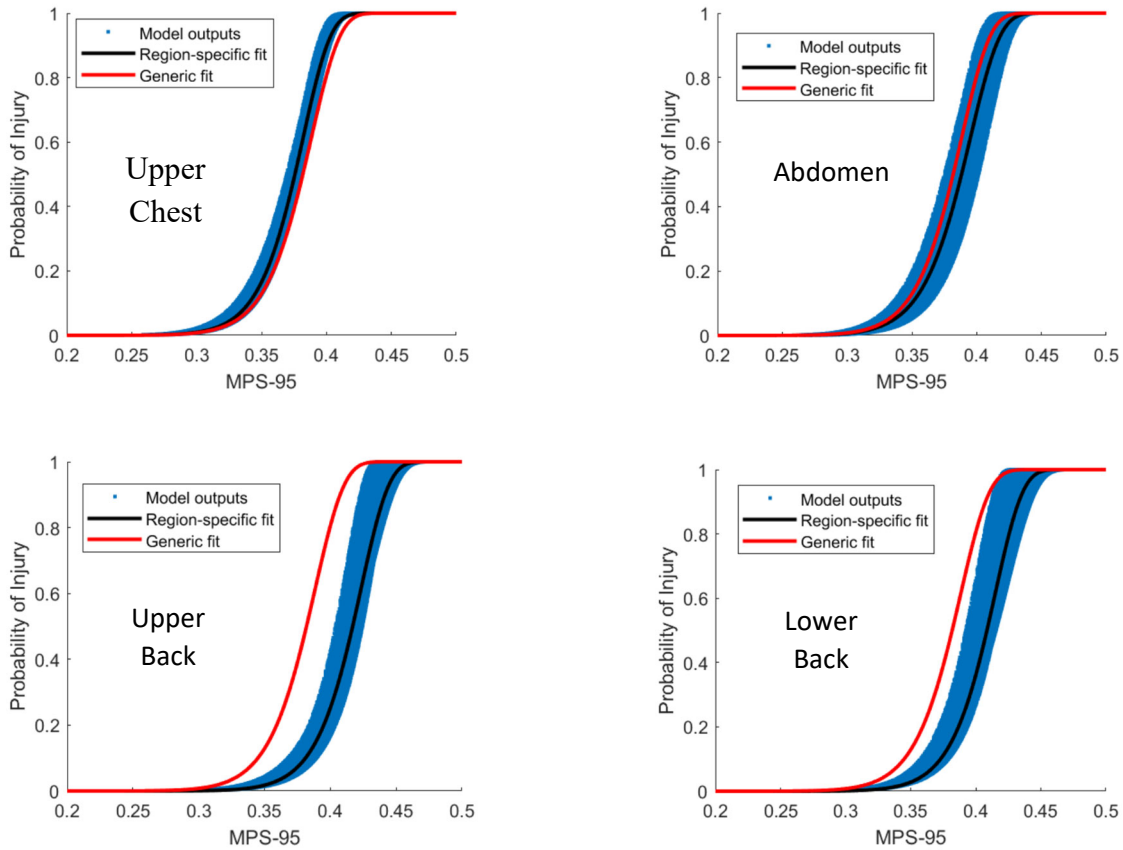


Figure 13. Injury risk vs. MPS-95. IRF based on regional skin thickness and separated by body region.

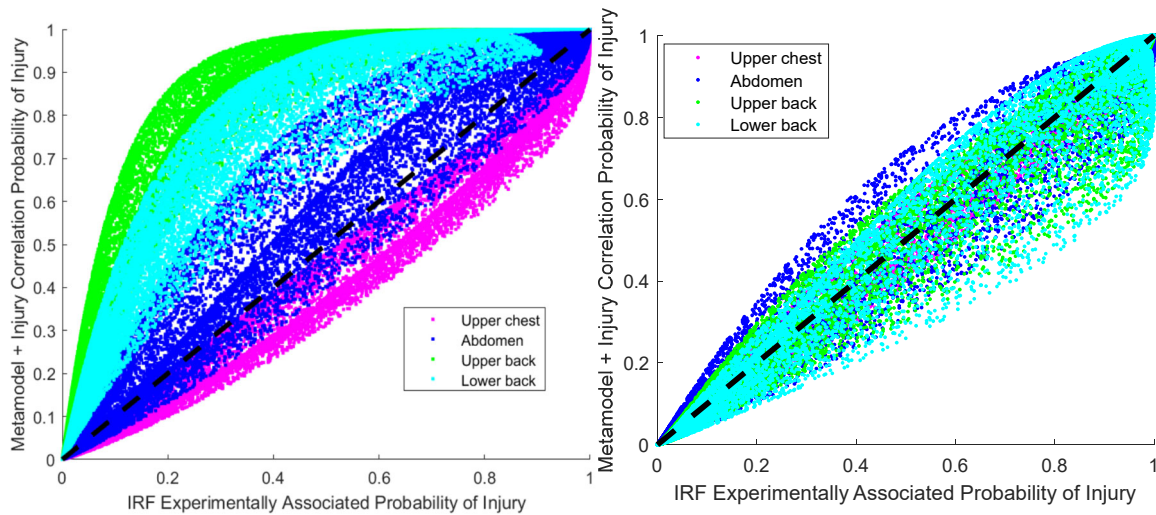


Figure 14. Model vs. experimental injury prediction without (left, reproduced from Figure 11) and with (right) region-specific injury correlations as shown in Figure 13. Region-specific injury correlations bring the results much closer to the 45° perfect-agreement line. To fully populate the right-hand plot, we extended the impact velocity range beyond that represented by the PMHS experiments.

3. Combine approaches 1 and 2. Statistically vary skin thickness appropriate to each body region when evaluating the IRF. Create a separate injury correlation for each body region. This would require region-specific skin thickness distributions.
4. Incorporate regional skin thickness variation into the FEM (and then the metamodel). This approach would attempt to reunify the injury correlations by generating a new metamodel incorporating skin thickness as an independent variable. (This would require running a new set of FEM simulations. We note that this assumes that the skin thickness can be readily adjusted within the shell element formulation of the FEM without remeshing.) In this construct, the FEM skin thickness would vary regionally, which would result in more accurate calculation of MPS-95, since we know that MPS-95 depends heavily on skin thickness. Recall that the underlying hypothesis is that MPS-95 is a material but not geometry dependent failure correlate. The need for multiple regional injury correlations in the previous two approaches was presumed to be due to the fact that MPS-95 was not being calculated in a comparable fashion in the different regions due to discrepancies between the anatomical skin thickness and the FEM skin thickness. The hope is that this more accurate MPS-95 calculation would obviate the need for different regional injury correlations. This should lead to a unified injury correlation that could be applicable to an arbitrary impactor/location/velocity. In this approach, the skin thickness in the injury risk function could either be set deterministically for each body region or varied in

accordance with appropriate anatomical/population statistics. Note that we could not compute a new scatterplot for this case because we only have the existing metamodel and are not equipped to run the FEM calculations.

In the near term, we recommend adopting approach number 3 and moving to approach number 4 when possible.

As a final note, we observe that all available data were used to produce the models with none held in escrow for independent validation. While this produces a model well-fit to the data, best practice is to independently validate the model using data held back from the model fitting procedure.

Appendix A. Detailed Discussion of Skin Penetration Mechanics

Background

In this appendix we describe mechanisms of skin penetration as they are understood and described in open literature publications. Our work was motivated by assessing challenges associated with predicting skin penetration depths from a blunt impact projectile. A literature search on both potential test data and damage models in human and animal skin revealed a large body of research on tensile response and associated tensile-loading-based skin damage. A comprehensive review of this subject can be found in [1, 2]. Unfortunately, this research is not applicable to the case of blunt impact skin penetration as a relatively large portion of the skin under the impactor is loaded in compression, and that is where the skin failure is likely to initiate in these cases. In order to predict when and how the impactor will penetrate the skin, appropriate criteria for critical levels of a well-defined skin damage correlate in compression need to be established.

We start with a brief summary of mechanics of skin response and damage accumulation in tension. This summary illustrates why criteria developed for skin loaded in tension may not be applicable to compressive loading, which we discuss in more detail next. Finally, we recommend that an experimental program needs to be designed to address this challenge.

Skin Response and Damage under Tensile Loading

Human skin displays nonlinear, heterogeneous, anisotropic, and viscoelastic mechanical properties, which are strongly influenced by the architecture and mechanical response of its microstructural components [2].

As it is documented in [3, 4], the mechanical response of dermis at different levels of complexity can be represented by the unraveling of the collagen fibers, which interact in ways that resemble a braided pattern, as is shown in Figure A-1.

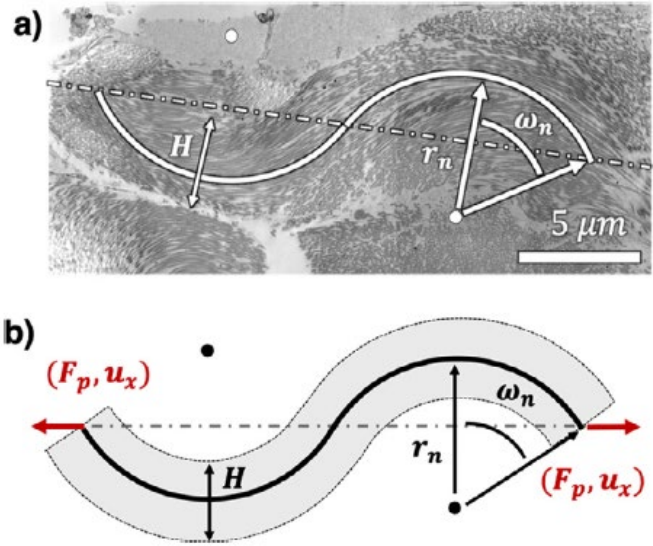


Figure A-1. Transmission electron microscopy (TEM) image of porcine skin (a) and its schematic representation (b), [3].

Under applied tensile loading, the collagen fibers exhibit frictional sliding, leading to increase in resistive forces with a dissipative component. In addition, the fiber bundles straighten and tend to arrange along the applied force direction.

The three stages of tensile skin response can be distinguished [5], as shown in Figure A-2.

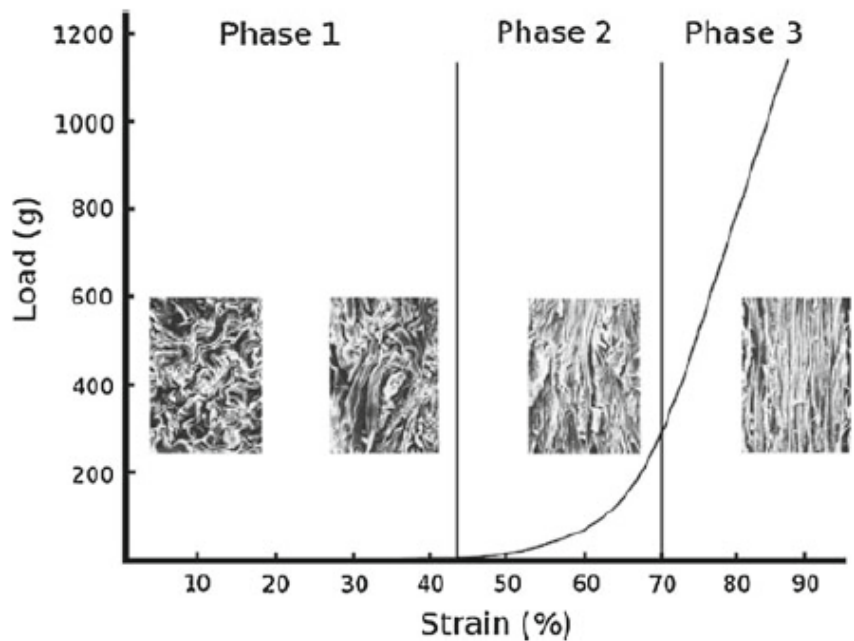


Figure A-2. Three stages of skin deformation under tension [5].

The initial phase is associated with low dynamic stiffness, and it corresponds to a gradual increase in stress with strain. This is thought to be due to the reorientation of fibers toward the axis of loading, followed by their straightening.

The second phase represents gradual stiffening when an increasing number of fibers becomes progressively aligned and begins to resist tension at different deformation stages, as reflected by the nonlinear mechanical response of skin.

The final phase is associated with the steep rise of stress with increasing strains. The majority of fibers are aligned and stretched at this stage, hence the overall mechanical response becomes dependent on mechanical properties of the fibers. Deformation beyond the final phase leads to yielding and rupture of the skin. The geometrical arrangement of fibers, strength of the fiber/matrix interface, and ultimate tensile breaking strength of fibers play a critical role in determining the onset of this irreversible damage accumulation.

Damage of skin is often referred to as tissue softening, which is represented by the curvature change of the stress vs. strain (stretch) curve. In a recent publication, a new damage model for the skin is described [6]. In this model, the skin is assumed to be anisotropic, hyperplastic, and incompressible. Additionally, this model includes families of the collagen fibers embedded in a matrix.

When relaxed, the collagen fibers are unstretched and wavy; under tension, the fibers are individually straightened until all of the fibers are recruited to resist the applied force. In human skin, the collagen fibers are grouped in large and small bundles, which are interconnected. The proposed model is essentially a modified version of the previously proposed Gasser–Ogden–Holzapfel (GOH) model, which uses a structure-based strain energy function and was developed to describe damage in arterial walls [7].

Irreversible skin damage and subsequent eventual failure occurs as the collagen fiber breaking limit is exceeded, when the fiber stretch is greater than 1.13–1.32, depending on the species, or when both the fiber and the matrix fail.

Skin Damage in Compression

We could not find any publications regarding the accumulation of damage when the skin is subjected to a high rate of compressive loading. Since most of the skin deformation in tension is based on the unraveling and eventual breaking of collagen fibers, the mechanics of squeeze and damage accumulation in skin under compression may be different from that under tension. (By analogy with textiles, consider crushing compression vs. stretching a sweater in tension.) A recent publication by Kong [8] described skin response under compression, but no data on skin failure in compression and associated mechanics-based skin damage correlates were reported.

Note that the collagen fibers in the skin are embedded in a host material (matrix) that is capable of transmitting internal forces. Uniaxial tensile loading produces tensile strain in the loading direction and leads to unilateral fiber alignment. Transverse compression, on the other hand, leads to one axis of compressive strain and two axes of tensile strain, with the tensile axes in the plane of the skin. This leads to stretching of fibers without the need for alignment, and likely changes the mechanics of damage accumulation as well as the failure criterion, such as maximum [principal] strain to failure.

Depending on how the force is transmitted from external loading to fibers (via the matrix) and different failure criteria for the matrix and the fibers, it is likely that compressive loading leads to different failure mechanisms compared to those in tension. In order to develop such compressive loading-based failure criteria, the following questions have to be addressed:

- Do fibers decouple from the matrix?
- Is the fiber failure due to the transforming of forces via deformation of the collagen matrix?
- Is the skin failure due to fiber pull-out that follows breaking fiber/matrix bonds, or fracture, or possibly both?

The matrix is likely to be the first point of failure. In the tensile loading case, the fibers may be directly loaded by the external force at the boundary. In compression, it can be presumed that tensile fiber strains can only occur via Poisson's ratio effect that leads to matrix expansion in transverse direction. In this case, questions to consider are:

- What happens to the fiber/matrix bond after the matrix fails?
- How much (if any) tensile load will be transmitted to fibers by continued compression of the failed matrix?
- Is the load to fibers transmitted via friction/viscous loading or the bond at the fiber/matrix interface?

Unfortunately, current publications do not provide enough to answer these questions.

Stresses in Skin under Blunt Impact Loading

In this section we consider how tensile or compressive loading relates to the more complex loading conditions experienced in an actual blunt projectile impact. While it is likely that there are regions of significant compressive stress in this case, the skin failure may not initiate in the region of direct compressive loading. Even if the compression generates different fundamental failure mechanisms for skin, skin loaded by a projectile impact is not in a state of pure uniaxial compressive loading.

A projectile is spatially confined, and it will likely have a contoured front, so there will be significant gradients in the loading conditions, e.g., potentially sharp transition areas between loaded and unloaded skin. Lateral boundary conditions could lead to significant shear zones with associated tensile stresses (not just tensile strain as in pure uniaxial compression). If these shear regions are responsible for the skin failure, then tensile models may be more readily applicable. However, if, as suggested earlier by the model described in [6], strain energy failure criteria are more appropriate, the compressive element of shear could be a significant factor in the determination of failure.

Boundary loading conditions will depend on impact locations. For instance, an impact in the abdomen, much like hitting a drum, might result in far-field lateral boundary conditions of nearly pure tensile stress. Deformation directly under the projectile would likely conform to the shape of the projectile front. Compressive loading at the skin surface as well as surface friction resistance to Poisson's-ratio-driven lateral expansion would both produce locally compressive stresses. Much like the Hertz contact problem, the contact area between the projectile and the skin would increase with loading. Thus, skin outside the initial contact region might be placed in tensile strain (the drum-like region), but, upon further loading, that skin might be brought into contact with the projectile with friction constraining further development of the surface state of strain. These conditions will likely lead to stress concentrations associated with edges of the projectile nose and regions of high shear stress near the edge of the projectile where the surface response changes from compressive to tensile. Furthermore, under the projectile nose, there will be a significant depth-wise gradient of compressive stress since the skin surface would be heavily loaded, but the interior muscle wall would be free of surface forces. In modeling such damage mechanisms, there would also be a challenge of deformation-matching at the skin-muscle interface.

In contrast, impacts over a hard substrate, such as the rib or tibia, would lead to quite different effects. In this case, rather than being pinched between the projectile and muscle in tension, the skin and muscle would be compressed between the projectile and the stiff bone. Having compressive stress throughout the soft-tissue depth could change the skin-muscle interface effects. Reduced freedom to conform to the progressing projectile would change the contact region, and, as such, higher loading could occur with this reduced contact area. Additionally, such impacts would result in a Hertz-type contact situation from within the bone as the bone loading of the soft tissue changes the footprint of the loading. The deformation resistance of the substrate would also prevent tensile loading of the surrounding soft tissue, leading to quite different lateral boundary conditions (tension-free). There could still be areas of high shear stress near the projectile boundaries due to transition from compressive stress to stress-free conditions. Friction from above and potentially below the site of impact could generate extrusion-type shear loading of the skin and muscle. Depending on the local curvature of the bones and the projectile, stress

concentrations could also be highest in interior portions of rigid substrate cases and thus, skin rupture could initiate from within.

In all these blunt impact loading conditions, there will be considerable tensile strains, some associated with tensile stresses and some due to Poisson's ratio effects. But there would also be regions of substantial compressive and shear strains and stresses.

Conclusions

Blunt impact loading generates considerable tensile, compressive, and shear strains as a result of applied tensile stresses as well as Poisson's ratio effects.

In a recent work, a Maximum Principal Strain (MPS) computed under tensile loading is applied for predicting probability of skin penetration [9]. The MPS values in the skin were obtained by considering 2-D shell elements and may not be applicable to the complex states of stress, ranging from tensile to high shear stresses.

The literature review shows that the damage criterion is most commonly based on strain energy formulation, rather than maximum principal strain [1, 6]. This is important because in the presence of significant compressive or shear loading, the strain energy may not be dominated by maximum uniaxial tensile strain.

To improve accuracy of predicting risk of skin penetration, we recommend that future tests validate that the failure criteria derived from the tensile tests apply to blunt impact conditions with significant compressive stress. The details of these tests (e.g., penetrator or indenter on skin coupon over known substrate) should be coupled with a FEM for computing internal tensile strains in skin loaded in compression at the time of failure, as reported by the experiments.

References

1. Lee, "Damage Models for Soft Tissues: A Survey." *J. Med. Biol. Eng.* (2016) 36:285–307
2. H. Joodaki and M. B. Panzer, "Skin Mechanical Properties and Modeling: A Review," *Proc IMechE Part H: J Engineering in Medicine*, 2018, Vol. 232(4) 323–343
3. Pissarenko et al., "Constitutive Description of Skin Dermis: Through Analytical Continuum and Coarse-grained Approaches for Multi-scale Understanding" 2020 *Acta Materialia Inc.* Volume 106, 1 April 2020, Pages 208-224
4. Pissarenko et al., "Tensile Behavior and Structural Characterization of Pig Dermis," *Acta Biomaterialia*, 86 (2019) 77–95

5. Jor, “Estimating Material Parameters of a Structurally based Constitutive Relation for Skin Mechanics,” *Biomech. Model Mechanobiol.* (2011) 10:767–778
6. W. Li and X. Lou, “An Invariant-Based Damage Model for Human and Animal Skins,” *Annals of Biomedical Engineering* (2016)
7. Gasser, T. C., R. W. Ogden, and G. A. Holzapfel, “Hyperelastic Modelling of Arterial Layers with Distributed Collagen Fiber Orientations,” *J. R. Soc. Interface* 3:15–35, 2006.
8. K.S. Kong, “Development of a Computational Model of Skin Damage under Blunt Impact to Investigate Skin Failure Threshold,” Ph. D., UVA, November 2020
9. D. Shedd et al., “Skin Penetration from Non-Lethal Munitions,” Final Technical Report, UVA Center for Applied Biomechanics, September 2021

Glossary

Injury correlation: one-to-one function relating the injury correlate, MPS-95, to the probability of skin-penetration injury.

Injury correlate: biophysical response variable used as the input to an injury correlation, in this case MPS-95

Injury risk function (IRF): empirically-derived relationship between impact conditions (velocity, diameter, shape, and skin thickness) and probability of injury

Metamodel: surface fit to the relationship between the FEM input conditions (velocity, diameter, shape, skin stiffness, adipose tissue stiffness) and FEM-computed MPS-95.

REPORT DOCUMENTATION PAGE*Form Approved*
OMB No. 0704-0188

The public reporting burden for this collection of information is estimated to average 1 hour per response, including the time for reviewing instructions, searching existing data sources, gathering and maintaining the data needed, and completing and reviewing the collection of information. Send comments regarding this burden estimate or any other aspect of this collection of information, including suggestions for reducing the burden, to Department of Defense, Washington Headquarters Services, Directorate for Information Operations and Reports (0704-0188), 1215 Jefferson Davis Highway, Suite 1204, Arlington, VA 22202-4302. Respondents should be aware that notwithstanding any other provision of law, no person shall be subject to any penalty for failing to comply with a collection of information if it does not display a currently valid OMB control number.

PLEASE DO NOT RETURN YOUR FORM TO THE ABOVE ADDRESS.

1. REPORT DATE March 2022		2. REPORT TYPE FINAL		3. DATES COVERED (From-To)	
4. TITLE AND SUBTITLE Skin Penetration Modeling Limitations and Opportunities				5a. CONTRACT NUMBER HQ0034-19-D-0001	
				5b. GRANT NUMBER	
				5c. PROGRAM ELEMENT NUMBER	
6. AUTHOR(S) Bhatt, Sujeeta B. Macheret, Yevgeny Teichman, Jeremy A. Swallow, Jessica G.				5d. PROJECT NUMBER DU-2-4273	
				5e. TASK NUMBER	
				5f. WORK UNIT NUMBER	
7. PERFORMING ORGANIZATION NAME(S) AND ADDRESS(ES) Institute for Defense Analyses Systems and Analyses Center 730 East Glebe Road Alexandria, VA 22305-3086				8. PERFORMING ORGANIZATION REPORT NUMBER IDA Document NS D-33040	
9. SPONSORING / MONITORING AGENCY NAME(S) AND ADDRESS(ES) Joint Intermediate Force Capabilities Office 3097 Range Road Quantico, VA 22134-5100				10. SPONSOR/MONITOR'S ACRONYM(S) JIFCO	
				11. SPONSOR/MONITOR'S REPORT NUMBER(S)	
12. DISTRIBUTION/AVAILABILITY STATEMENT Approved for public release; distribution is unlimited (20 July 2022).					
13. SUPPLEMENTARY NOTES					
14. ABSTRACT The University of Virginia (UVA) built a model for estimating the risk of significant injury due to skin penetration. All such models utilize approximations. The Johns Hopkins University Applied Physics Laboratory (JHU/APL) plans to implement this model into the JIFCO Blunt Impact modeling suite. In this document, we characterize some shortcomings and limitations JHU/APL's planned implementation of the UVA skin penetration model by examining both the theoretical considerations of the model construct and on UVA's own experimental results. We also suggest a number of potential future enhancements to improve the accuracy of the model predictions.					
15. SUBJECT TERMS blunt impact human effects; mechanics of skin penetration; skin penetration injury correlation; skin penetration modeling					
16. SECURITY CLASSIFICATION OF:			17. LIMITATION OF ABSTRACT	18. NUMBER OF PAGES	19a. NAME OF RESPONSIBLE PERSON
a. REPORT Uncl.	b. ABSTRACT Uncl.	c. THIS PAGE Uncl.			Burgei, Wesley
			SAR	29	(703) 432-0899